

# Characterizing the Product Crystals from a Mixing Tee Process

R. Mohanty, S. Bhandarkar,  
B. Zuromski, R. Brown, J. Estrin

Department of Chemical Engineering  
University of Rhode Island  
Kingston, RI 02881

The classical theory of nucleation has been acceptably well developed, particularly as it pertains to vapor-liquid transformation in pure systems. When liquid solution-solid crystal transformations are considered the theory is still applied, typically, but with less confidence. Perhaps the best measure of the extent to which one can accept classical theory for these latter systems is provided by a study of the experimental results of Nielsen (1969, 1971). He carried out homogeneous nucleation studies for a variety of ionic crystal-aqueous solution systems. He was able to show reasonable agreement between classical theory and experiment for some salts (e.g., 2,2 electrolytes), while success was mixed for others. The major goal of this work is the characterization of the crystals which are produced through homogeneous nucleation by the Nielsen process. In order to do this, a preliminary experimental study of the process is required to identify the mechanisms by which the observed product is formed. This paper describes work serving to standardize the experimental procedure.

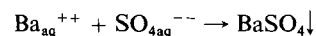
## Experimental

Precipitation experiments were carried out using a modified Nielsen apparatus, Figure 1. Nielsen's original apparatus was activated by two syringes operating in parallel, each of capacity 5 mL. These operated simultaneously to force the two reactant streams to intimately mix in a downstream tee. The device provided a sample of the precipitate for subsequent study—primarily the counting of the product crystalline entities; it also permitted a measure of the reaction or induction time  $t_i$ , i.e., the period elapsed between the time of mixing and the visually determined onset of precipitation. The general idea behind this was to mix reactant solutions rapidly so that the precipitation mechanisms occurred from a well-mixed homogeneous solution. The mixing occurred in a specially designed mixing tee whose characteristic mixing time was estimated to be about one millisecond. Obtaining a particular relationship between the number

of particles,  $N$  vs. initial supersaturation,  $S_0$ , ensured that homogeneous nucleation had occurred.

The apparatus modification involved in this work included a larger volume of reagents, say a maximum of 525 mL, and a mixing tee of simpler configuration. The motivating idea behind this latter change was to enable easy characterization of the tee in the event that future scale-up and modifications were to be considered. The tubing sizes given in Figure 1 are about the same as those used by Nielsen (1961). The larger quantities of reactants were desirable as the goals of the experiments included providing product crystals in sufficient quantities for more elaborate characterization and further processing. Plexiglass vessels D served to contain the reactants under air pressure as they were fed to the mixing tee. In Figure 1, C is the pressure gauge, B, the pressure regulator and A, an in-line filter; vessels D were fed from vessels I whose contents were transported through filters G (0.22  $\mu\text{m}$ ) by the diaphragm pump G.

The goals of the specific work being described here were to provide the basic data required for future design of the apparatus for a variety of systems and to obtain some insight into the mixing-reaction characteristics of the basic process. For this latter goal the precipitation of  $\text{BaSO}_4$  from aqueous solution was selected as Nielsen had shown this to be relatively well-behaved. The precipitation reaction is:



The product was found to be insensitive to the other ions present as by products of the reaction ( $\text{NaCl}_{\text{aq}}$  and  $\text{HNO}_{3\text{aq}}$  were present in different experiments) with no consequence regarding results. Our data for solutions of stoichiometric proportions are shown in Figure 2. Linear behavior on the coordinates shown is indicative of homogeneous nucleation. The leveling off of the data with increasing abscissa values (decreasing supersaturation) is due to the dominance of heterogeneous nucleation in the domain of lower supersaturations.

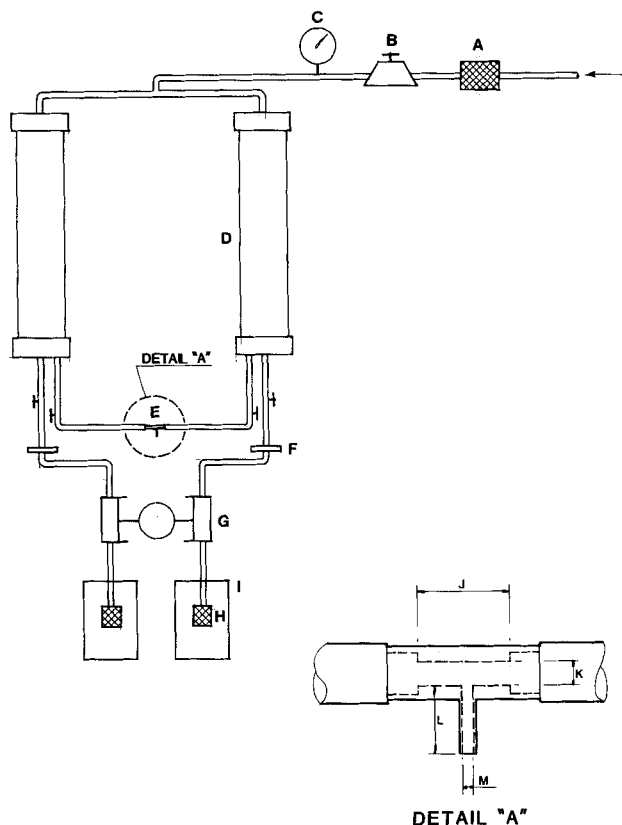


**Figure 1. Mixing configuration.**

Dimensions are:  $J = 10.0$  mm;  $K = 3.4$  mm;  $M = 1.9$  mm;  $L = 3.0$ ,  $9.0$ ,  $90.0$  mm.

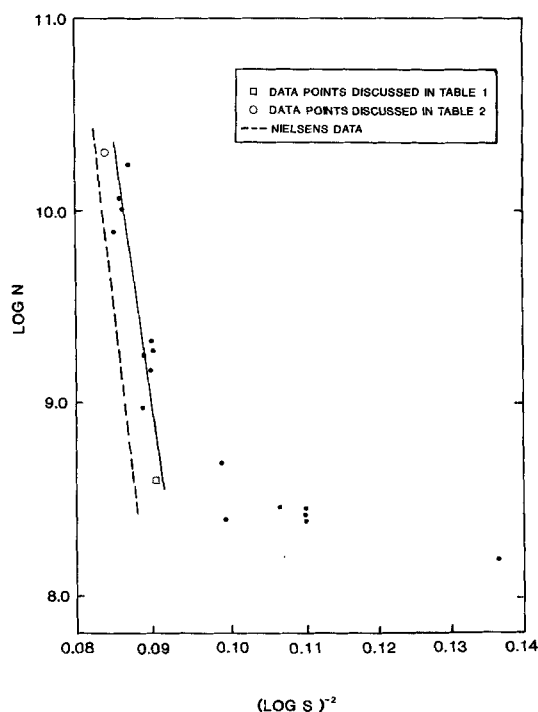


**Figure 2. Experimental data graphed on  $\log(S_o)^{-2}$  vs.  $\log(N)$  coordinates ( $N$  in number/mL).**

These data were obtained using standard run conditions:  $9.0$  mm jet length;  $N_{Re} = 24,000$ ;  $\Delta P = 310$  kPa.

Experiments were conducted at room temperature; deliberate operation well beyond the range of daily room temperature fluctuations gave results showing no additional scatter. The experimental procedure involved simultaneously discharging the two reactant solutions (about  $300$  mL of each reactant) from the vessels  $D$  in Figure 1. The discharge was done under pressure so that the two jets of the reactants would impinge and rapidly mix in the mixing tee  $E$ . The initial suspension discharged was discarded. Samples for analysis were taken after steady state had been reached and they represented only the middle portion of the entire discharge (about  $50$  mL). The operation of this preliminary device is ballistic in nature so that the full control of the two flows was not attainable; absolute flow rates were "tuned" to be the same from the feed containers and were estimated from the time required to discharge the liquid reactant solutions. The total flows from each chamber were the same (to  $\pm 10$  mL in  $300$  mL) or the run was considered unacceptable. (An apparatus under construction for continuation of this research will not suffer from these deficiencies.) The sampling procedure consisted of discharging jet suspension into a known volume of  $0.02\%$  wt. gelatin solution ( $50$  mL into  $500$  mL typically, but depending on the  $S_o$  of the run involved). The gelatin served to stabilize the suspension and the dilution arrested or reduced the growth rate of the crystals. A sample of the diluted suspension was introduced onto a microscope slide for general observation and counting. Samples for electron microscopy were obtained by placing a drop of the product suspension onto a carbon coated,  $200$  mesh copper grid. The excess solution on the grid was removed by absorption upon placing the grid onto a filter paper. It was then dried so that only crystals were retained on the carbon film. Both these transfers were made within  $1$  minute of the run and the influence of solution based secondary mechanisms such as Ostwald ripening in these samples was unlikely.

## Results

Figure 3 shows a typical micrograph obtained using optical microscopy from a "standard" run. The calculated reaction or induction time  $t_1$  (Nielsen, 1969) is about a millisecond or less depending on the initial supersaturation. This is the estimated

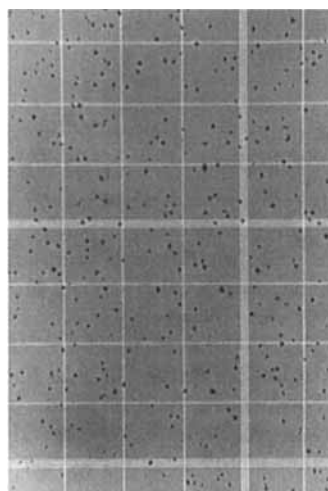


**Figure 3. Optical micrograph, short tee product,  $N_{Re} = 24,000$ ,  $S_o = 2,000$ , distance between grid lines is  $0.05$  mm.**

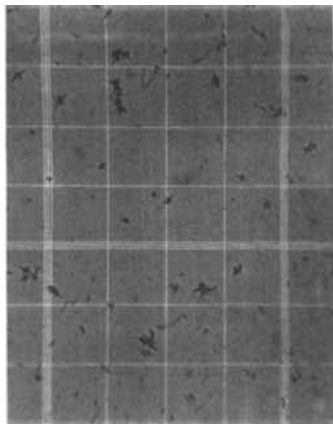


**Figure 4.** Optical micrograph, mixing done manually,  $S_o = 2,000$ , distance between grid lines is 0.05 mm.

time period over which nucleation has completely taken place. One millisecond is the characteristic mixing time  $t_m$  for this physical configuration. This was Nielsen's value (1969) and was also estimated using the shear slab model of Angst et al. (1982). The induction time is sensitively dependent upon the supersaturation and chemical system, and the formula used to calculate  $t_i$  was derived from considerations of classical nucleation and diffusion controlled growth (Nielsen, 1969). Figure 4 shows a micrograph, same magnification, of the product developed from manually stirred reactants. The reactant concentrations were the same as those used in preparation of the product of Figure 3. This was done by pouring the two reactant solutions simultaneously into a beaker. The particle count is of most significance—Figure 3 yielding a value of  $4.0 \times 10^8$  entities per ml and Figure 4 about  $8.0 \times 10^6$ . The count and the appearance of the entities in Figure 3 were not influenced by mixing as discussed later, while those in Figure 4 were likely influenced by inadequate mixing. These counts were made directly from the micro-

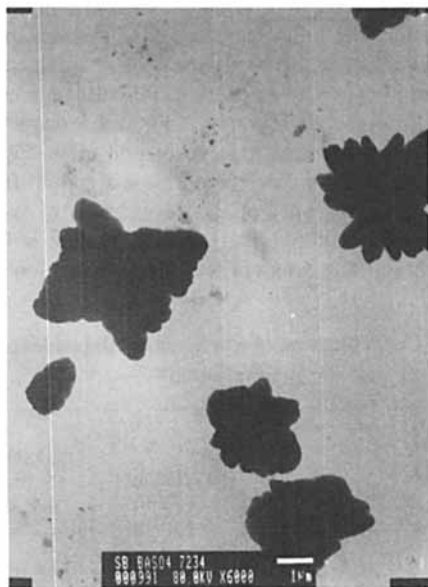


**Figure 5.** TEM, short tee product,  $N_{ro} = 24,000$ ,  $S_o = 2,000$ .

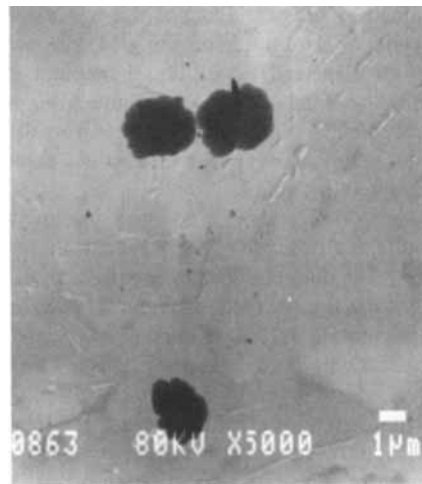


**Figure 6.** TEM, long tee product,  $N_{ro} = 13,500$ ,  $S_o = 2,000$ .

scope using a calibrated slide (hemacytometer), onto which a known volume of liquid is placed and which contains an imprinted grid to be used as a reference during counting. Figure 5 shows an electron micrograph (TEM) of the material from a run made under the same conditions as Figure 3. These micrographs, Figures 3 and 5, were typical of all "short" arm runs—i.e. mixing arm length of 9.0 mm.

Figure 6 shows product obtained using the mixing tee with the "long" mixing arm—90.0 mm in length. These are typical of all long tee results. Figure 7 gives corresponding results for a mixing tee with essentially no arm; its length consisted only of the wall thickness of the tubing—3.0 mm ("zero" tee). The individual particles seen in these figures were confirmed to be single crystals of  $\text{BaSO}_4$  by electron diffraction with no evidence of dislocations. This indicated that these are primary crystals and not agglomerates. Some apparent agglomeration seen in Figure 6



**Figure 7.** TEM, zero tee product,  $N_{ro} = 24,000$ ,  $S_o = 2,000$ .

can be explained by the overlaying of the crystals during sampling and drying of the sample on the grid. However, the particles were well dispersed in the liquid medium used during counting with the optical microscope, Figure 3. Figures 5, 6 and 7, enable direct comparison among products from different mixing arm lengths. Operating parameter values associated with these are presented in Table 1.

Table 1 shows long, short and zero mixing arm length counting results as a function of the Reynolds number.  $N_{Re}$  was based on the inner diameter of the mixing arm of the tee,  $d$ . Count values  $N$  are the key results sought. Residence time  $\Theta$  and turbulence microscale values (Kolmogorov)  $\lambda$  are also given along with each  $N$  value as a matter of interest. Two features are evident—there is an order of magnitude difference between counts from the short and zero mixing arms, and the long mixing arm results; and there is little sensitivity of the counts to Reynolds numbers. This latter observation seems evident from the short and “zero” tee runs; no significant differences were evident among the long tee results, at least over the limited Reynolds number values involved. (Actually the Reynolds number values referred to have little significance as such when comparing the flow character among the three tees. In at least two of the three arms fully developed flow was not attained and in the “zero” arm tee the diameter was different from the others.)

## Discussion

When the characteristic mixing time  $t_m$  of the operation is greater than the characteristic reaction time  $t_1$ , the reactants are not fully mixed when precipitation has been initiated. Whatever the detailed mechanism may be, this leads to the conclusion that supersaturation is depleted before the number of nuclei has attained a magnitude equal to that for the  $t_m \ll t_1$  case. Before mixing is complete, the first nuclei have grown to sizes which significantly deplete the supersaturation. Since nucleation is more sensitive than growth to level of supersaturation, its average effective rate is diminished. This causes a larger sized, smaller particle concentration product in the poorly mixed case. Figures 3 and 4 demonstrate this phenomenon. As the  $N$  results

from the zero mixing arm are about the same as those from the short arm, one would expect that mixing effects are not present. That is, the greatest influence of inadequate mixing should be evident for changes in residence times (or mixing periods)  $\Theta$  for small  $\Theta$ , e.g., 0.1 to 0.5 ms (zero and short tee respectively) as compared to  $\Theta \gg 0.5$  ms (long tee). Yet Table 1 shows  $N$  which are contrary to this: the greater changes in  $N$  occur for short tee-long tee operations. This change in  $N$ , therefore, does not occur because of incomplete mixing prior to nucleation.

Most of the data depicted in Figure 2 are for supersaturations  $S_o$  greater than  $S_o = 2,000$ . These data at  $S_o > 2,000$  graph linearly on the coordinates of Figure 2, in accordance with nucleation theory, implying that mixing influences are minimal. The maximum  $S_o$  at which experimental counting was feasible was about 2,700. When  $S_o$  is raised to still higher values, such as above 3,000, the particle size does not decrease with increase in  $S_o$ . This is contrary to the observations for  $S_o$  results that were countable. However, this is consistent with a falling off of the rate of increase of  $N$  with  $S_o$  as was noted by Nielsen which he attributes to mixing as one possibility.

Table 2 gives counting results for long and short tees and two Reynolds numbers at two supersaturation levels. The effect of inadequate mixing on nucleation would be expected to be greater at greater  $S_o$ . This is because the characteristic reaction time  $t_1$  is smaller at greater  $S_o$  and the presence of some degree of rate control by mixing mechanisms would be revealed, were they present, by variation in  $N$  with  $N_{Re}$ . But there is little effect of  $N_{Re}$  on  $N$  at  $S_o = 2,700$ , suggesting practically adequate mixing before nucleation. From the above arguments it may be concluded that mechanical mixing plays a minor role at most, in the  $S_o = 2,000$  range in determining the value of  $N$ . However, mixing becomes a factor in controlling the rate of nucleation above  $S_o$  greater than about 3,000 for our system.

The difference in count levels between short and long arm lengths is more marked in Table 1 than the differences noted above. This is possibly due to either mixing improvement effected by the greater length (residence time) or to secondary nucleation. From the discussion above it would appear that mixing effects upon precipitation kinetics are minimal. To support this conclusion, the influence of another mechanism, e.g., secondary nucleation, has to be shown to be of significance so that the increase in count by an order of magnitude is convincingly explained. From the micrographs in Figures 5, 6 and 7, it is clear that secondary nucleation does occur and increasingly so with residence time in the mixing arm. This is apparent from consideration of the appearance of the degradation of faceting with residence time in the figures (long tee product is less faceted than the others). The extent of secondary nucleation is more evi-

**Table 1. Number of Particulates from Mixing Tee**  
 $S_o = 2,000$  ( $t_1 = 0.5$  ms)

$N_{Re}$	Tee Size		
	$L = 3.0$ mm	$L = 9.0$ mm	$L = 90.0$ mm
2,400	$\Theta$ ms	7.8	—
	$\lambda$ $\mu$ m	—	—
	$N \times 10^{-9}$ /mL	0.11	—
3,200	$\Theta$ ms	4.0	36.0
	$\lambda$ $\mu$ m	6.3	7.5
	$N \times 10^{-9}$ /mL	0.17	2.5
7,900	$\Theta$ ms	1.5	14.0
	$\lambda$ $\mu$ m	4.4	5.1
	$N \times 10^{-9}$ /mL	0.11	2.6
13,500	$\Theta$ ms	0.8	8.0
	$\lambda$ $\mu$ m	3.4	4.0
	$N \times 10^{-9}$ /mL	0.25	2.7
24,000	$\Theta$ ms	0.1	0.5
	$\lambda$ $\mu$ m	5.8	2.2
	$N \times 10^{-9}$ /mL	0.3	0.35
47,000	$\Theta$ ms	0.1	—
	$\lambda$ $\mu$ m	4.3	—
	$N \times 10^{-9}$ /mL	0.4	—

**Table 2. Concentration of Particulates Dependence on  $S_o$  and Tee Length**

Short Tee	13,500	24,000
$S_o \setminus N_{Re}$	( $\Theta = 0.8$ ms)	( $\Theta = 0.5$ ms)
2,000( $t_1 = 0.50$ ms)	$2.2 \times 10^8$ /mL	$4.0 \times 10^8$ /mL
2,700( $t_1 = 0.15$ ms)	$2.1 \times 10^{10}$ /mL	$2.1 \times 10^{10}$ /mL
Long Tee	10,000	13,500
$S_o \setminus N_{Re}$	( $\Theta = 1.0$ ms)	( $\Theta = 0.8$ ms)
2,000( $t_1 = 0.50$ ms)	$2.6 \times 10^9$ /mL	$2.7 \times 10^9$ /mL
2,700( $t_1 = 0.15$ ms)	$2.1 \times 10^{10}$ /mL	$2.2 \times 10^{10}$ /mL



Figure 8. SEM, short tee product,  $N_{R_0} = 24,000$ ,  $S_0 = 2,000$ .

dent on comparison of the scanning micrographs (SEM) of Figures 8 and 9. SEMs showing the zero tee product (not included) are very similar to that shown in Figure 8. The product crystals have morphologies which involve platelets of many orientations. From these figures it is clearly evident that the attrition may be productive of secondary nuclei, enough so to effect an order of magnitude change in count.

Other observations are relevant to the above arguments. These pertain to the sizes of the particles from each of the long and the short arm tees. The long arm yielded particles in the size range of 1 to 1.5  $\mu\text{m}$ , which were included in the count using optical microscopy. Also there were a large number of fines ( $<0.1 \mu\text{m}$ ) which were not counted but clearly observed using electron microscopy. The short arm particles were mostly 2 to 4  $\mu\text{m}$  with some 20% or so between 4 and 6  $\mu\text{m}$ . There were a small number whose sizes were about 1  $\mu\text{m}$  and hardly any fines ( $<0.1 \mu\text{m}$ ). That is, fines when significantly present, accompany a suspension of smaller particles. For this reason the fines in the long tee product are believed to be a consequence of fragmentation of the primary particles rather than due to continued nucleation in the long tee. Furthermore, according to theory continued nucleation at the lower supersaturations in the downstream regions of the long tee is unlikely. The former description that larger particles are the result of inadequate mixing and smaller ones indicate well mixed reactants does not hold here; the smaller sized product from the long tee is clearly bimodal in nature and there is no explanation for this within the classical nucleation theory.

The difference in morphologies and sizes between the long tee and the two shorter tees in all likelihood occurs because of addi-



Figure 9. SEM, long tee product,  $N_{R_0} = 13,500$ ,  $S_0 = 2,000$ .

tional residence time in the long tee. [We tacitly take the character of the particles at  $X = 9.0 \text{ mm}$  ( $L$  for the short tee) to be the same for the short and the long tee.] If one compares the mass of solid which should be ideally deposited for depletion of nearly all supersaturation and the mass of the observed particles,

$$c_o = (nN/M)(\rho_s \pi (d_p/2)^2 t) \quad (1)$$

where  $t$  is the thickness of the disc and  $n$  is the number of full circular discs equivalent to the mass of a typical crystal entity. Here disc geometry is used as the basis to calculate the volume of a particle which is constituted of platelets.

Using the long tee results, for which

$$S_0 = 2,000 \rightarrow c_o = 0.02 \text{ mol/L,}$$

$$n = 2, d_p = 1.5 \mu\text{m}, t = 0.075 \mu\text{m.}$$

Equation 1 then gives

$$0.02 = ?(2 \times 2.5 \times 10^9 / 233.4)(4.5 \times 10^3 \times \pi (7.5 \times 10^{-5})^3 / 10)$$

$$0.02 > 0.012$$

As expected, this says that the mass calculated using the observed particle size is less than the theoretical maximum. The comparison is much closer in the case of the zero tee, where

$$n = 2, d_p = 4.0 \mu\text{m}, t = 0.075 \mu\text{m.}$$

Then,  $0.02 > 0.018$ .

This difference in the two calculated masses supports the significance of the fines in the long tee product, which were not counted. The zero tee was selected for this comparison over the short tee because of the near monodispersity of the zero tee product. This latter material balance is believed to hold for the short tee as well because of the similarities of the product from the two tees.

The difference in numbers between shorter tee and long tee products is discussed below. Computer modelling shows that when  $X = 9.0 \text{ mm}$  (length of the mixing arm of the short tee),  $S = 0.6 S_0$ . In the long tee, therefore, if secondary nuclei are formed at about  $X = 9.0 \text{ mm}$ , the supersaturation that still exists can cause the secondary nuclei to grow. Thus the countable particles in the long tee product would be primary particles which were eroded and secondary nuclei which have grown. In the short tee the stream exiting from the mixing arm has the above stated supersaturation. This supersaturation is essentially depleted by growth during the travel of the jet from the end of the mixing arm to the diluent. Only during travel within the mixing arm does erosion of the larger particles occur.

In addition to the length of tee effects, the erosion of the primary particles also depends on their sizes. At higher supersaturations, the primary nuclei are much more numerous and are consequently smaller after depletion of supersaturation. As is seen from Table 2 and confirmed by electron microscopy, there was no evidence of breakage in the long tee using  $S_0 = 2,700$ , where the primary particle size is very small ( $<1.0 \mu\text{m}$ ), say, compared to the turbulence microscale. This supports the conclusion that the difference in the long and the short arm product sizes at smaller  $S_0$  is due to attrition effects. The ratio of particle

counts from long and short tees, which is held as the meaningful parameter, is unity within experimental error for these  $S_o = 2,700$  runs.

Such experiments using the long tee and the short tee were carried out for the system  $\text{Ca}(\text{OH})_2$ -water. For this system it was found that the crystals grew only to submicron sizes within the tee. The long and the short tee gave products for the  $\text{Ca}(\text{OH})_2$  system with identical particle concentrations. The implication is that the attrition in the tee is significant when the crystal sizes become comparable to the turbulence microscale ( $1\text{ }\mu\text{m}$ ) within the tee.

## Conclusions

Precipitation studies using a modified Nielsen apparatus and the  $\text{BaSO}_4$ -water system yielded homogeneously nucleated particles as expected. When these attained the micron size range in the mixing arm they served as sources of new nuclei through secondary mechanisms. This was borne out by the apparent attrition of the larger particles yielded by the longer mixing arm and the associated larger number of particles.

## Acknowledgment

We acknowledge the support provided by the NSF-Grant No. CBT8502409.

## Notation

- $B$  = preexponential factor in the expression for homogeneous nucleation
- $c_o$  = concentration of the precipitating compound after mixing, before precipitation.
- $d$  = diameter of mixing arm; mean ionic diameter
- $d_p$  = average particle dimension as measured from electron micrographs
- $D$  = diffusion coefficient
- $J_o$  = nucleation rate per unit volume of solution;  $B \exp(-\Delta G^*/kT)$

- $L$  = length of mixing arm
- $M$  = molecular weight of solute
- $N$  = number of particles per unit volume of solution (as counted by optical microscopy)
- $N_{Re}$  = Reynolds number
- $Q$  = volumetric flowrate
- $S$  = instantaneous supersaturation
- $S_o$  = initial supersaturation of mixed reactants
- $t$  = thickness of disc equivalent to a  $\text{BaSO}_4$  crystal platelet
- $t_i$  = characteristic reaction time (when obtained experimentally)
- $t_m$  = characteristic mixing time
- $t_1$  = estimated calculated characteristic reaction time =  $15^{2/5} (16\pi J_o (2D^3 c_o v)^{1/2})^{-2/5}$  (Nielsen, 1969)
- $v$  = mean ionic volume
- $X$  = distance in the mixing arm from the entrance

## Greek letters

- $\Delta G^*$  = free energy change associated with the formation of a critical nucleus
- $\Delta P$  = measured pressure drop across the apparatus
- $\epsilon$  = power dissipation per unit mass.  $\Delta PQ/\rho d^2 L/4$
- $\Theta$  = residence time in the mixing arm
- $\lambda$  = Kolmogorov microscale;  $(\nu^3/\epsilon)^{1/4}$
- $\nu$  = kinematic viscosity
- $\rho$  = density of solution
- $\rho_s$  = density of the solid precipitate

## Literature Cited

- Angst, W., J. R. Bourne, and R. N. Sharma, "Mixing and Fast Chemical Reaction: IV," *Chem. Eng. Sci.*, **37**, 585 (1982).
- Nielsen, A. E., "Kinetics of Precipitation," Pergamon (1964).
- Nielsen, A. E., and O. Sohnel, "Interfacial Tensions Electrolyte Crystal-Aqueous Solution, from Nucleation Data," *J. Crystal Growth*, **11**, 233 (1971).
- Nielsen, A. E., "Nucleation and Growth of Crystals at High Supersaturation," *Kristall und Technik*, **4**, 17 (1969).
- , "Homogeneous Nucleation in Barium Sulfate Precipitation," *Acta. Chem. Scand.*, **15**, 441 (1961).
- , personal communication.

Manuscript received Feb. 5, 1988, and revision received June 10, 1988.